Full title:
Effective polyploidy causes phenotypic delay and influences bacterial evolvability

Short title:
Phenotypic delay by effective polyploidy in bacteria

Lei Sun[1,], Helen K. Alexander[1,2,*], Balazs Bogos[1], Daniel J. Kiviet[3,4], Martin Ackermann[3,4], Sebastian Bonhoeffer[1,#]*

[1]*Institute of Integrative Biology, ETH Zürich, Universitätstrasse 16, Zürich, Switzerland.*
[2]*Current address: Department of Zoology, University of Oxford, South Parks Road, Oxford OX1 3PS, UK*
[3]*Institute of Biogeochemistry and Pollutant Dynamics, ETH Zürich, Universitätstrasse 16, Zürich, Switzerland*
[4]*Department of Environmental Microbiology, Eawag, Swiss Federal Institute of Aquatic Science and Technology, Überlandstrasse 133, Dübendorf, Switzerland.*

[*]shared first authors
[#]corresponding author: seb@env.ethz.ch

Whether mutations in bacteria exhibit a noticeable delay before expressing their corresponding mutant phenotype was discussed intensively in the 1940s-50s, but the discussion eventually waned for lack of supportive evidence and perceived incompatibility with observed mutant distributions in fluctuation tests. Phenotypic delay in bacteria is widely assumed to be negligible, despite lack of direct evidence. Here we revisited the question using recombineering to introduce antibiotic resistance mutations into *E. coli* at defined time points and then tracking expression of the corresponding mutant phenotype over time. Contrary to previous assumptions, we found a substantial median phenotypic delay of 3-4 generations. We provided evidence that the primary source of this delay is multifork replication causing cells to be effectively polyploid, whereby the presence of wild-type gene copies transiently masks the mutant phenotype in the same cell. Using mathematical models, we showed that this multigenerational delay has profound consequences for mutation rate estimation by fluctuation tests, standing genetic variation and evolutionary adaptation to rapidly shifting selection pressure such as antibiotic treatment. Overall, we have identified phenotypic delay and effective polyploidy as previously overlooked but essential components in bacterial evolvability, including antibiotic resistance evolution.

Introduction

As genetic mutations appear on the DNA, their effects must first transcend beyond the RNA- and protein-level before resulting in an altered phenotype. A substantial phenotypic delay could have major implications for evolutionary adaptation, in particular when selection pressures can change on a time scale that is short relative to this delay, as may be the case for selection by antibiotics. The duration of phenotypic delay is an old but nearly forgotten question in microbiology(1,2). Luria and Delbrück were interested in the delay as they expected it to affect the mutant distribution in the fluctuation test in their seminal work on the random nature of mutations(1). They argued that if a mutant clone expressed its phenotype after G generations, then phenotypic mutants should be observed in populations in groups of 2^G. Frequent observations of single-mutant populations however suggested $G \approx 0$. They thus concluded that the phenotypic delay is negligible(2). This has remained the *modus operandi*(3), despite the fact that molecular cloning protocols imply a significant delay

as they require a waiting time typically longer than a bacterial generation to express new genetic constructs(4).

To quantify the phenotypic delay more directly, the time point of occurrence of a mutation in a cell needs to be known, which has only become possible with modern methods of genetic engineering. Here we use a recombineering approach to introduce mutations in *E. coli* within a narrow time window and find a remarkable phenotypic delay of 3-4 generations for three antibiotic resistance mutations. We identify the underlying mechanism as effective polyploidy, which reconciles the long phenotypic delay with Luria and Delbrück's observations. Investigating the consequences of effective polyploidy and phenotypic delay, we find that mutation rate estimates based on fluctuation tests need to be adjusted for ploidy. Moreover, resistance mutations that occur after exposure to antibiotics are much less likely to survive due to the multi-generational phenotypic delay, and thus pre-existing mutations become a much more important contributor to survival.

Results

Mutations in bacteria exhibit multi-generational phenotypic delay

To quantify phenotypic delay we introduced each of four mutations at a specified time-point in *E. coli*, with an optimized recombineering protocol (Methods). Three mutations (RifR, NalR, StrepR) confer antibiotic resistance(5); the fourth mutation (lac+) enables lactose prototrophy(6) (Table S1). After introduction of the mutations the cells grew continuously without selection and were sampled over time. Sampled cells were subjected to "immediate" versus "postponed" selection to quantify, respectively, the frequencies of current phenotypic mutants and of genotypic mutants (that contain at least one mutant gene copy and eventually have some phenotypic mutant descendants), with their ratio called phenotypic penetrance (Fig. 1A). Phenotypic delay is quantified as the time in bacterial generations to reach 50% phenotypic penetrance.

Surprisingly, all three resistance mutations showed significant phenotypic delay at two selective concentrations of their respective antibiotic (Fig. 1B). Reaching 50% phenotypic penetrance required 5-6 generations of post-recombineering growth. The frequency of genotypic mutants increased over the first 1-2 generations but eventually declined (Fig. 1D). The transient increase may reflect the time window of introduction of the mutations. Discounting the first two generations, a phenotypic delay of 3-4 generations remains to be explained.

Effective polyploidy is the primary source of phenotypic delay

Phenotypic delay could result from multiple factors. Firstly, it could arise from the gradual replacement of wild-type proteins by mutant proteins following mutagenesis. Time may be required for sufficient protein turnover before the mutant phenotype can manifest. Another possibility is that cells are effectively polyploid due to multifork replication(7,8). Recombineering incorporates the mutation into only one or some of the chromosomes(9), comparable to when natural mutations emerge. This yields effectively heterozygous cells that could produce both wild-type and mutant proteins from different chromosomes, which may prevent the onset of the mutant phenotype. Three generations could be the minimal time needed for a cell with one mutant copy out of eight chromosomes (comparable to previous estimates(7)) to produce the first homozygous mutant carrying only mutant alleles. Effective polyploidy is also compatible with the observed decline in genotypic mutant frequency (Fig. 1D), because heterozygous mutants produce both mutant and wild-type descendants, such that the

frequency of cells carrying at least one mutant gene copy will decline until all cells are homozygous.

To quantify the contribution of effective polyploidy, we used a *lacZ*-reporter assay to visualize heterozygous mutants. We constructed three reporter strains with a disrupted *lacZ* gene inserted close to each resistance target gene and restored it through recombineering (Table S2). Genotypic mutants were visualized by plating on indicator media where lac+ and lac- cells become blue and white, respectively. Heterozygous mutants generate sectored colonies while homozygous mutants generate blue colonies, thus indicating the frequency of homozygous mutants amongst all genotypic mutants (Fig. 1F). Comparing the estimated proportion of homozygous reporter mutants with the corresponding phenotypic penetrance of the resistance mutation reveals that phenotypic delay can be fully explained by effective polyploidy for NalR at 2xMIC and for RifR (Fig. 1C). Homozygosity precedes phenotypic penetrance by about 0.5 generations for NalR at 8xMIC and one generation for StrepR, suggesting that here additional protein turnover may be involved. These results also imply that these resistance mutations are genetically recessive to antibiotic sensitivity, which corroborates previous studies based on co-expression assays(10,11).

We scored the frequency of lac+ phenotypic mutants on lactose-limited medium. The ability to metabolize lactose is dominant to its inability(6). Since any cell containing a lac+ allele can metabolize lactose and eventually form a colony, phenotypic penetrance, as expected, was always at 100% (Fig. 1E), indicating that the observed phenotypic delay of resistance mutations is not an artifact of our protocol. We also investigated the effects of chromosomal locations on recombineering and the subsequent phenotypic delay (Suppl. Text and Fig. S1).

Effective polyploidy causes asymmetrical inheritance of mutations

A further testable prediction of effective polyploidy is that inheritance of mutant alleles is asymmetrical: heterozygous mutants are expected to produce both wild-type and mutant offspring. For mutations with intermediate dominance, offspring progressing towards mutant homozygosity should show an increasingly mutant phenotype, while others show a transient phenotype as they inherit no mutant genes and their mutant proteins are diluted over subsequent divisions. Phenotypic delay would manifest as the time such mutations need to reach full phenotypic expression. To test this prediction, we repaired a disrupted *YFP* gene with recombineering, creating fluorescent mutants where the fluorescence intensity depends on the number of functional copies of this gene. We then tracked fluorescence as an intermediate-dominant phenotypic trait using single-cell imaging. As expected we observed fully, transiently and non-fluorescent offspring lineages from recombineering-treated cells (Fig. 2A-C, Supplementary Movie), consistent with effective polyploidy. Furthermore, fluorescence in mutant lineages increased monotonically and reached maximal intensity almost two generations after forming homozygous mutants (Fig. 2C). This additional delay could be due to protein folding(12). These results provide direct visual support that effective polyploidy underlies phenotypic delay. A similar pattern has been observed previously in *E. coli* with fimbrial switching, a genetic modification that involves inversion of a promoter sequence on the bacterial genome(13).

Integrating polyploidy and phenotypic delay into the Luria-Delbrück fluctuation test

Fluctuation tests are widely used to estimate bacterial mutation rates by counting mutants exhibiting a selectable phenotype, where selection is typically applied to

stationary phase cells(14), which are expected to be polyploid(8,15). Polyploidy should affect the appearance of mutants in the fluctuation test(16,17), but this factor is not generally taken into account in analyses and the extent of error introduced by applying standard methods to effectively polyploid populations remains unclear.

When a mutation arises in an effectively polyploid cell, the first homozygous mutant descendant must appear as a single cell in the population (Fig. S2). Therefore in contrast to earlier interpretations(1), the frequent observation of singletons in the mutant distribution does not invalidate the existence of a substantial phenotypic delay. Furthermore, since heterozygous cells carrying recessive mutations do not exhibit the mutant phenotype, i.e. cannot form colonies on selective plates in the fluctuation test, these unobserved mutants should result in an underestimation of the mutation rate. Incidentally, the phage or antibiotic resistance mutations typically used in fluctuation tests are recessive(10,11,18).

We investigated the effect of polyploidy on observed mutant distributions and hence estimated mutation rates, for both dominant and recessive mutations, by simulating fluctuation tests. Our simulation model assumed fixed effective ploidy at the target, by doubling and equally dividing chromosome copies upon division according to a model of segregation in *E. coli* (Methods). From simulated cultures we counted phenotypic mutants given either a completely dominant or a completely recessive mutation, assuming instant protein equilibration, and estimated mutation rates using standard methods(14,19,20). Under our model, ploidy level c has two effects relative to monoploidy: (i) it increases the number of mutation targets and thus the per-cell mutation rate by a factor c, and (ii) it generates initially heterozygous mutants that after a delay of $\log_2 c$ generations produce one out of c homozygous mutant descendants (Fig. S3).

The mutation rate estimate at the mutational target can be compared to the actual per-copy rate μ_c and per-cell rate $c \cdot \mu_c$ used in the simulations (Fig. 3A-B). When c=1 (monoploidy), as the standard method assumes, the estimate indeed reflects the per-copy or (equivalently) per-cell rate. For c>1 the estimate is higher for dominant than for recessive traits. Surprisingly, for recessive traits, the estimate tends to coincide with the per-copy rate μ_c regardless of ploidy. For dominant traits, the estimate lies between the per-copy and per-cell rates, with confidence interval size increasing with ploidy. These patterns are robust across a range of parameter values (Fig. S4) and can be explained mathematically by the effects of polyploidy on the distribution of mutant counts (Suppl. Text, Fig. S5), which turns out to match the standard model with rescaled mutational influx in the case of a recessive trait (Fig. 3C), but fundamentally differs for a dominant trait (Fig. 3D). Thus, for more commonly used recessive traits, estimates reflect mutation rates per target copy, which can be scaled up to per genome copy. This could explain why per-nucleotide mutation rates estimated from different targets do not differ significantly, despite differences in target location that potentially influence their copy number(21). However, neglecting polyploidy underestimates the total influx of *de novo* mutations in a population.

Polyploidy and phenotypic delay impact bacterial evolvability under selection

Effective polyploidy has important consequences for evolutionary adaptation, both through the aforementioned increased influx of mutations and the masking of recessive mutations' phenotype. Masking of deleterious recessive mutations is expected to increase their frequency in the standing genetic variation (SGV) and yield transiently lower, but eventually higher, mutational load in a fixed environment(22,23). This higher standing frequency could promote adaptation to new environments should these

mutations become beneficial. However, in an environment where mutations are beneficial, masking their effects should hinder adaptation. Previous theoretical studies addressing these conflicting effects of ploidy on adaptation(22,24) have not been linked to bacteria, nor have they specifically considered the chance of evolutionary rescue, i.e. rapid adaptation preventing extinction under sudden harsh environmental change (e.g. antibiotic treatment).

Rescue mutations may pre-exist in the SGV and/or arise *de novo* after the environmental shift during residual divisions of wild-type cells. The source of rescue mutations has implications for the optimal approach to drug treatment(25) and the preservation of genetic diversity following rescue(26). We first derived the frequency of mutants carrying costly mutations in the SGV at mutation-selection balance, with a population genetics model incorporating effective polyploidy and chromosome segregation in bacterial cells (Fig. S6). This yielded analytical expressions confirming that polyploidy increases the frequency of a recessive mutant allele by masking its cost in heterozygotes. In contrast, the total mutant allele frequency is independent of ploidy if the mutation is dominant (Table S4 and Fig. S7). Next, we developed a stochastic branching process model to evaluate the probability of extinction of pre-existing or *de novo* mutations. Combining these components yielded expressions for the probability of population rescue from SGV, P_{SGV}, and from *de novo* mutations, P_{DN}, elucidating dependencies on ploidy, dominance, and other model parameters (Suppl. Text).

In the recessive case, if phenotypically wild-type cells cannot divide in the new environment (e.g. a perfectly effective antibiotic), then P_{SGV} is independent of ploidy (Fig. S8), reflecting the constant frequency of pre-existing phenotypically mutant homozygotes (Table S4). This result is consistent with our above findings for fluctuation tests. If division of wild-type cells is possible (e.g. imperfect antibiotic efficacy) then P_{SGV} increases with ploidy, since heterozygotes may produce additional homozygous mutant descendants. On the other hand, P_{DN} decreases with ploidy, as *de novo* mutations require more cell divisions until segregation is complete and the mutant phenotype is expressed, which turns out to outweigh the increase in mutational influx (Suppl. Text). Thus, although the overall probability of rescue remains similar as ploidy increases (Fig. S8), rescue is increasingly from SGV rather than *de novo* mutations (Fig. 4A). The effect can be dramatic, with the ratio P_{SGV}/P_{DN} increasing approximately ten-fold with each doubling of ploidy for a highly (95%) effective antibiotic and other realistic parameters. These qualitative patterns are robust to variations in the model parameters, though the quantitative effect size varies (Fig. S9-10). For dominant mutations, on the other hand, both P_{SGV} and P_{DN} increase with ploidy, and their relative contributions can show more complex patterns (Fig. 4B and S8-10).

Discussion

The phenotype of a bacterial mutation cannot manifest instantaneously. Here we thus asked two questions: how large is this phenotypic delay and what is its primary cause? We found a delay of 3-4 generations in the expression of three recessive antibiotic resistance mutations in *E. coli* and provided evidence that effective polyploidy is its primary cause.

Polyploidy is often regarded as a transient property limited to fast-growing bacteria, but this view has been challenged in recent years. Though ploidy tends to be higher during exponential growth (up to eight or 16 partial chromosome copies)(7), even during stationary phase *E. coli* cells contain typically four and up to eight complete chromosome copies(8). Environmental stresses can also induce multinucleated, polyploid cell filaments(27), in which adaptive mutations must overcome phenotypic

delay before allowing population survival in deteriorating environments. A recent study exposing bacteria to low doses of the antibiotic ciprofloxacin showed that resistant bacteria can only emerge from mono-nucleated offspring cells that bud off from a long multinucleated cellular filament(27). This observation can be explained by masking of the mutant phenotype in polyploid, heterozygous cells. Furthermore, obligate polyploid bacterial species ranging from free-living bacteria to clinically relevant pathogens have been discovered across six phyla(15,28,29). This has for instance been recognized as a confounding factor in metagenomic studies of bacterial community structure by marker-gene-based analysis(28). Therefore, we argue that polyploidy is broadly relevant for bacteria, and will generally result in phenotypic delay of recessive mutations.

Dominance and polyploidy (whether effective or obligate) together affect the mutant distribution observed in fluctuation tests and require reinterpretation of mutation rate estimates. Most notably, since fluctuation tests typically utilize recessive antibiotic resistance mutations, their estimates reflect the per-target-copy mutation rates, but not per-cell rates. This outcome is consistent across ploidy levels, which may be influenced by media conditions. Therefore we expect that the results of studies consistently using fluctuation tests with a given recessive mutation to compare mutation rates across different conditions, e.g. (30), are not affected by polyploidy. Absolute estimates of mutation rate by fluctuation tests, however, need to be interpreted with caution as the per-cell rate depends on the ploidy level. Ploidy is expected to affect sequencing-based methods of mutation rate estimation similarly (Supplementary section 4), implying that absolute mutation rates more generally need to be revisited.

The effects of polyploidy on number of mutational targets and phenotypic delay influence the evolutionary potential of populations to escape extinction under sudden environmental change such as antibiotic treatment. In particular, we showed that recessive rescue mutations are increasingly likely to come from the standing genetic variation as ploidy increases. While we examined rescue via single mutations, if multiple mutations with different dominance were available, populations at different ploidy levels may tend to evolve via different pathways(31). Models developed thus far have assumed constant ploidy, whereas future modeling efforts could incorporate the dynamically changing and environment-dependent nature of bacterial ploidy. Finally, while we exclusively considered chromosomal mutations, mutations on plasmids, particularly those with high copy number(32), should show similar effects, although segregation patterns and hence time to achieve homozygosity are likely to differ. Given the manifold implications of a multigenerational phenotypic delay, we argue that effective polyploidy and the resulting phenotypic delay are essential factors to consider in future studies of bacterial mutation and adaptation.

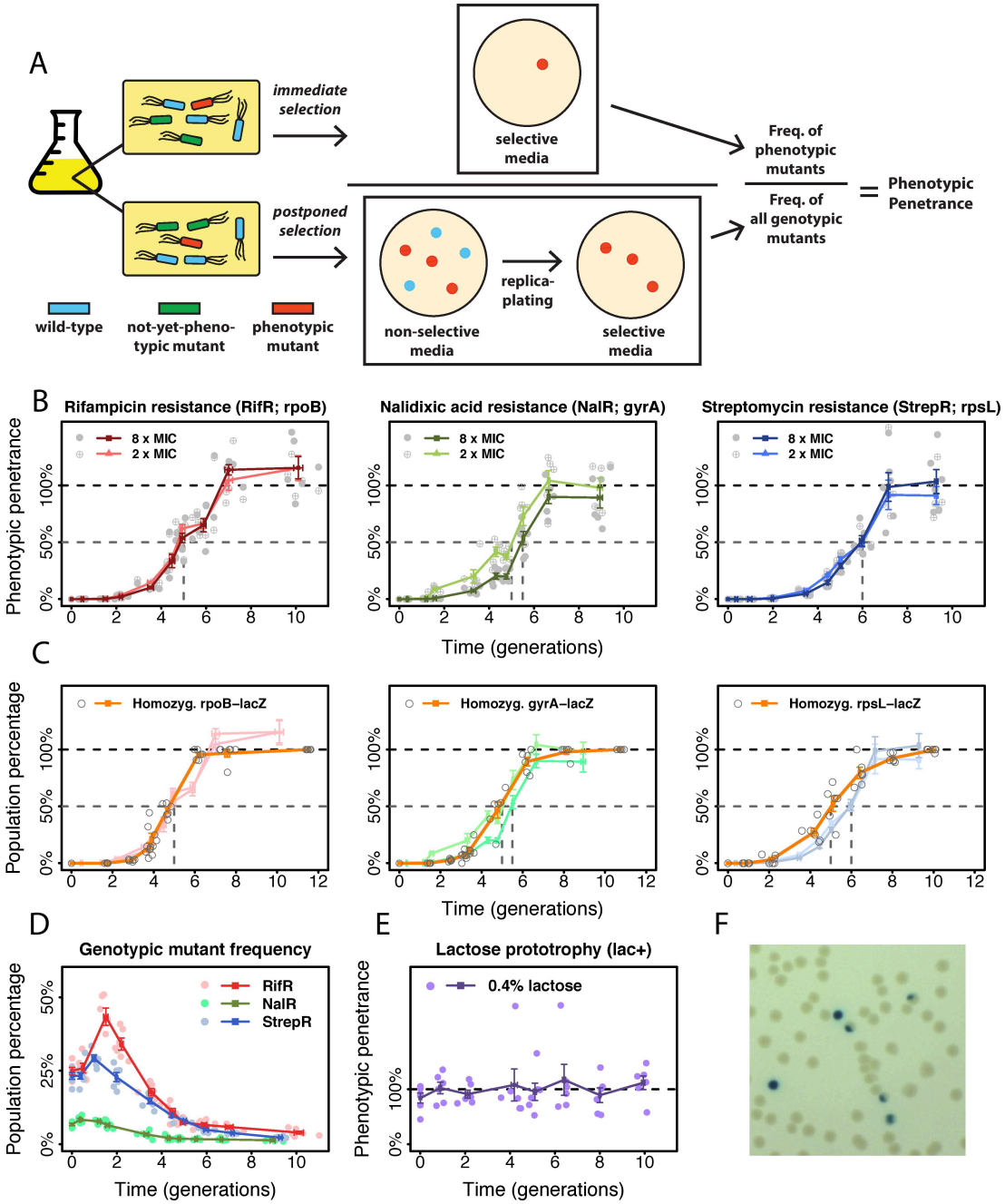

Figure 1. Phenotypic delay in *E. coli*. (A) Schematic illustration of the quantification of phenotypic penetrance. (B): phenotypic penetrance (mean ± SE; n = 6) over time for three antibiotic resistance mutations. Gray dashed lines: time at 50% phenotypic penetrance. (C): Frequency of homozygous mutants among all mutants (orange) for the three resistance mutations assessed by *lacZ*-reporter constructs (*rpoB-lacZ*, *gyrA-lacZ*, *rpsL-lacZ*), overlaid with their respective phenotypic penetrance. (D): Genotypic mutant frequency for the resistance mutations. (E): Phenotypic penetrance of the lactose prototrophy (*rpsL-lacZ*). (F): Colonies founded by homozygous (blue) and heterozygous (sectored) lac+ mutants.

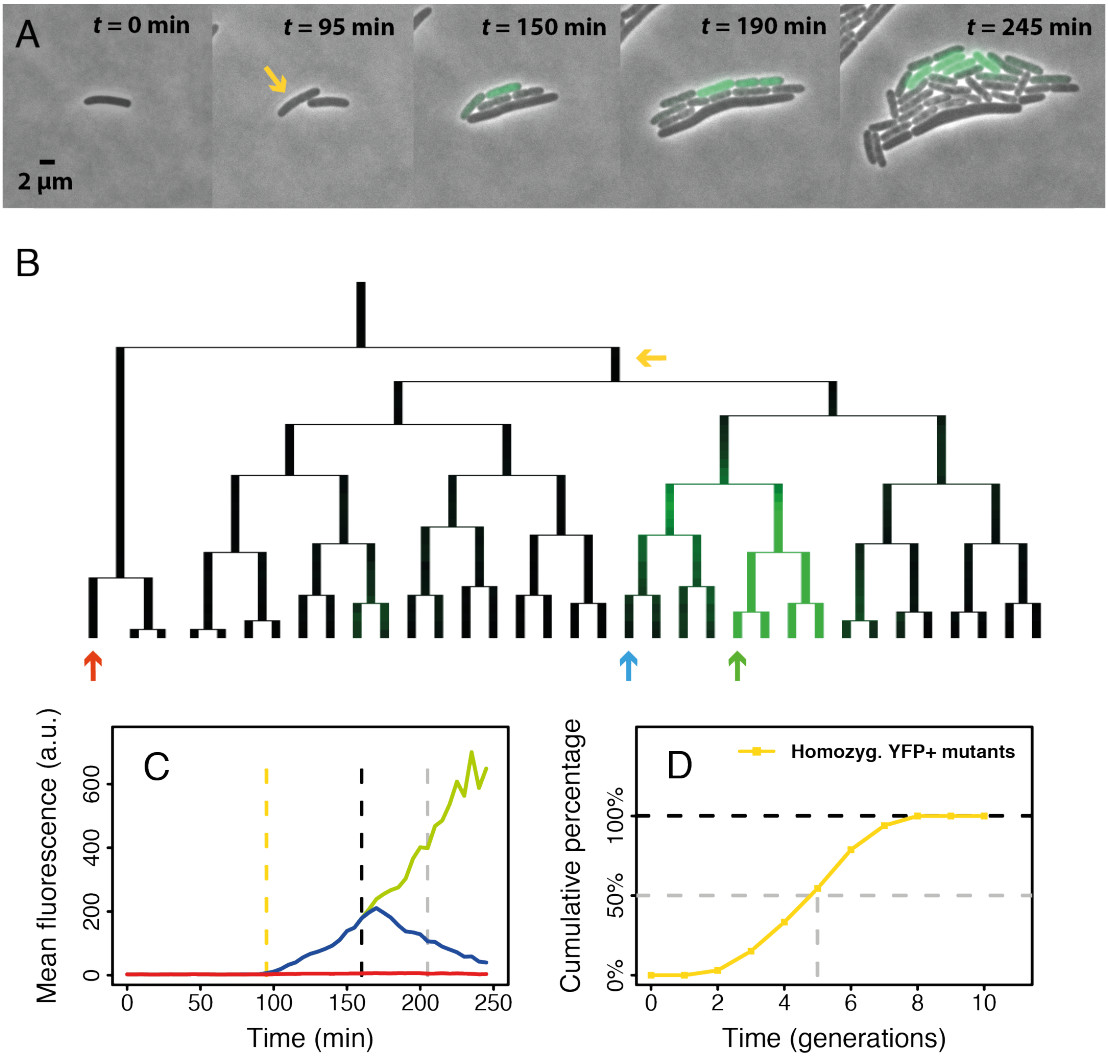

Fig. 2. Single-cell analysis of fluorescent mutants. (A): Overlay of phase-contrast and fluorescence images showing a micro-colony containing fluorescent mutants (see also Supplementary Movie). Yellow arrow: the first cell showing significantly higher fluorescence than background in the given frame. Accounting for the time required of YFP protein folding and maturation, the ssDNA integration must have happened before the first cell division. (B): Genealogy of the aforementioned micro-colony. The yellow arrow indicates the cell in (A) while the remaining arrows indicate three lineages in which fluorescence was quantified. (C): YFP expression history of three lineages in (B) showing fully, transiently and non-fluorescent phenotypes (green, blue and red). Yellow dashed line: onset of fluorescence; black: emergence of the first homozygous mutant; grey: its first division. (D): Time to form homozygous mutants in 25 micro-colonies. It took a median of five generations until a homozygous mutant emerged, consistent with our *lacZ*-reporter study. The data is based on two separate experiments.

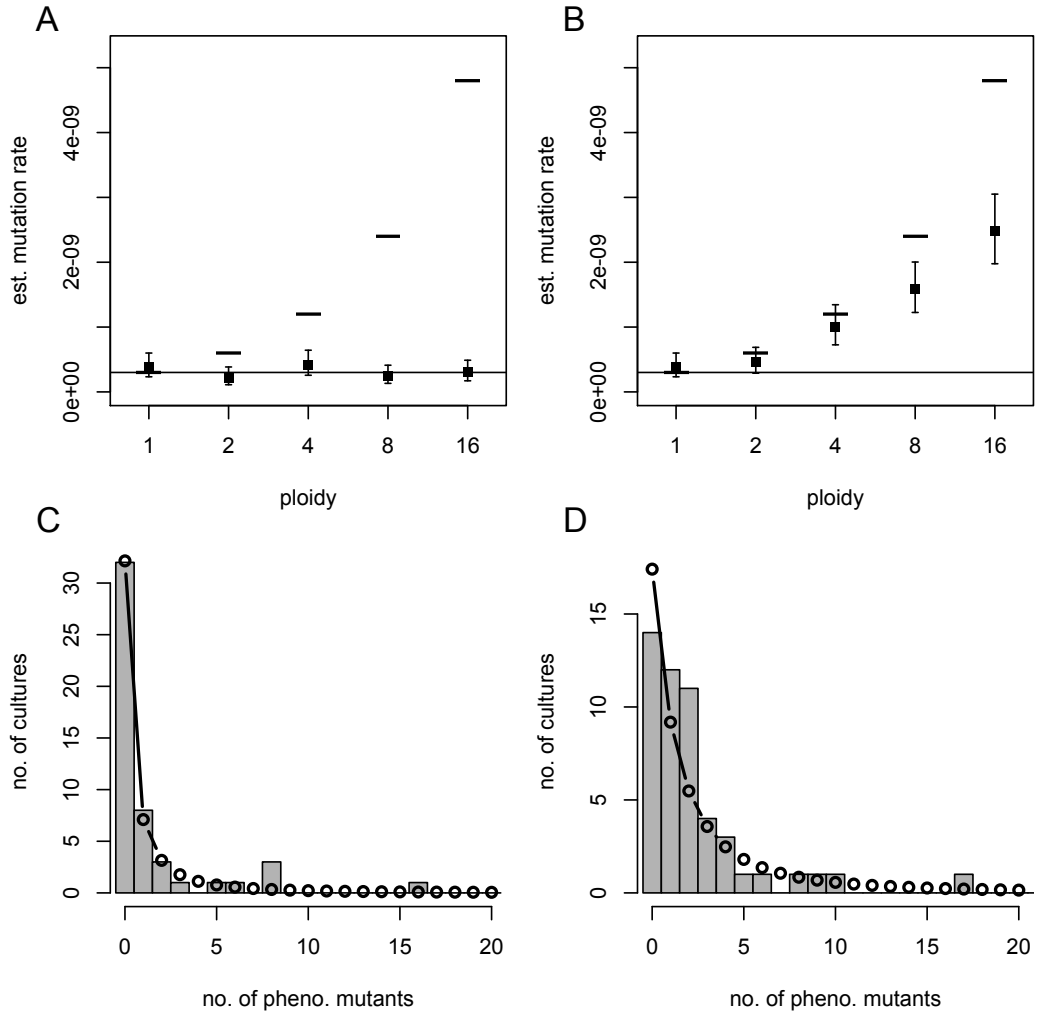

Fig. 3. Simulated fluctuation tests. Mutation rate estimates (maximum likelihood estimate, MLE, filled squares; and 95% confidence intervals, error bars) from 50 simulated parallel cultures at each ploidy (c), with constant mutant interdivision time, assuming either a recessive (A) or dominant (B) mutation. The lower solid line and upper dashes indicate the per-copy ($\mu_c = 3 \times 10^{-10}$) and per-cell ($c \cdot \mu_c$) mutation rates, respectively, used for simulation. For c=4 and recessive (C) or dominant (D) mutations, the observed mutant count distribution (histogram) is compared to that predicted by the standard model parameterized by the MLE mutation rate (connected points).

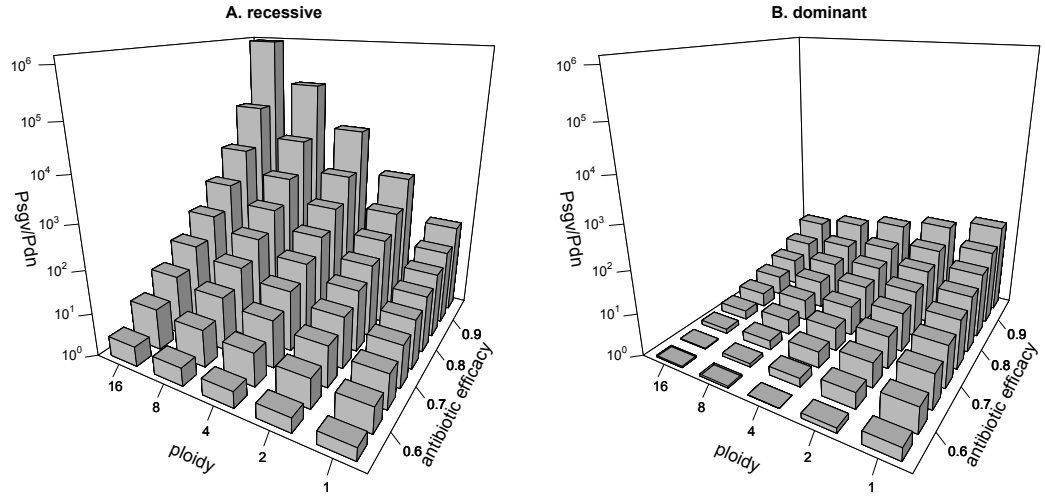

Fig. 4. Probability of evolutionary rescue from standing genetic variation versus *de novo* mutations. The ratio of the probability that at least one mutation from the SGV survives in the new environment (P_{SGV}) to the probability that at least one mutation arises in the new environment and survives (P_{DN}) is plotted as a function of ploidy and "antibiotic efficacy". The latter is a measure of the harshness of the new environment, defined as the probability that a phenotypically wild-type (antibiotic-sensitive) cell dies before dividing. Note that the ratio is always >1 for this parameter set and increasing with ploidy in the recessive case (A), but in the dominant case (B) the ratio can drop below 1 (i.e. $P_{\mathrm{SGV}} < P_{\mathrm{DN}}$) and tends to be decreasing with ploidy, though this trend reverses at some parameter ranges. The remaining parameters (see Supplementary Text for details) are fixed: antibiotic efficacy against a resistant cell of 0.1; mutational cost in the old environment, s = 0.1; population size when antibiotic treatment starts, N = 2 x 10^8; and per-copy mutation rate, μ_c = 3 x 10^{-10}.

Materials and Methods

Bacterial strains, antibiotics and media: All experiments were performed with strains derived from the wild-type *E. coli* MG1655 strain. A complete list of strains can be found in Table S2. Cells were grown at 30°C in LB or in M9 media with 0.4% lactose. Antibiotics were purchased from Sigma-Aldrich. To prepare stocks, rifampicin was dissolved in DMSO to 100 mg/ml; nalidixic acid was dissolved in 0.3M NaOH solution to 30 mg/ml; streptomycin and ampicillin were dissolved in MilliQ water to 100 mg/ml and filter sterilized. Rifampicin, streptomycin and ampicillin stocks were kept at -20°C while nalidixic acid was kept at 4°C. 100 mg/L ampicillin was used for maintaining the pSIM6 recombineering plasmid. All antibiotic agar plates were prepared fresh before every experiment.

MIC determination: The MICs of rifampicin, streptomycin and nalidixic acid were determined by broth dilution method in LB and found to be 12 mg/L, 12 mg/L and 6 mg/L, respectively.

High efficiency recombineering: Our recombineering protocol was adapted from previous studies(9,33). To ensure reproducibility, a detailed step-by-step protocol is provided in the Supplementary Text (Section 1). In brief, *E. coli* harboring pSIM6 plasmids were grown into early exponential phase before heat-activation at 43°C for 10 minutes to express the recombineering proteins. Activated cells were then repeatedly washed in ice-cold MilliQ water to remove residual salts. 50 µl of concentrated salt-free cell suspension was then mixed with ~200 ng of ssDNA before electroporation at 1.8 kV/mm. Immediately after electroporation cells were resuspended in LB and recovered for 30 min at 30°C. After this initial recovery cells were pelleted, then resuspended in fresh LB to continuously grow at 30°C for subsequent phenotyping.

Quantification of phenotypic delay of mutations: From the resuspended population ~2% of cells were sampled hourly for the first 10 hours and then at 24 and 48 hours. The sampled populations were appropriately diluted for optimal plating onto selective and non-selective plates. Population size and thus generations was estimated from CFU on non-selective plates. To score the frequency of genotypic mutants we replica-plated all colonies from the non-selective plates to selective plates at each sampled time point. The frequency of genotypic mutants, F_g, was determined by the fraction of colonies from non-selective plates that could grow after replica-plating onto selective plates. The frequency of phenotypic mutants, F_p, was determined by the ratio of CFU from direct plating on selective plates versus CFU on non-selective plates. Phenotypic penetrance is defined as $P = F_p / F_g$. Phenotypic delay was then quantified as the time point at which phenotypic penetrance reaches 50%.

Quantification of homozygosity: To quantify mutant homozygosity, i.e. the fraction of homozygous mutants among all genotypic mutants, we developed a *lacZ*-based visual assay. We constructed bacterial strains with a *lacZ* gene disrupted by a nonsense point mutation (E461X)(6) and inserted the broken *lacZ* within 5 kb of each antibiotic resistance target gene. These strains were subjected to recombineering with an ssDNA carrying the reverse point mutation (X461E) that restored the lac+ phenotype. The resulting phenotypic mutants were selected on M9-lactose media. Phenotypic mutants become blue on permissive media containing IPTG and X-gal(4). Heterozygous mutants with mixed lac+/lac- alleles form blue/white-sectored colonies, whereas homozygous mutants form entirely blue colonies (Fig. 2E). Counting sectored (s) and non-sectored (n) blue colonies, we determined mutant homozygosity as $f_{\mathrm{hom}} = n/(s+n)$. Comparing f_{hom} to the phenotypic penetrance P thus indicates to what extent phenotypic delay is attributable to effective polyploidy. All the colony counting was performed using

CellProfiler(34).

Single-cell observations: We constructed a strain with a constitutively expressed *YFP* gene disrupted by three consecutive stop codons. Recombineering corrected the stop codons and after electroporation and 30 min recovery at 30°C, 1 µl of appropriately diluted cell suspension was pipetted onto a small 1.5% UltraPure Low Melting Point agarose pad. After drying the pad for 1 minute it was deposited upside down in a sealed glass bottom dish (WillCo Wells, GWST-5040). Time-lapse microscopy was performed with a fully automated Olympus IX81 inverted microscope, with 100X NA1.3 oil objective and Hamamatsu ORCA-flash 4.0 sCMOS camera. For fluorescent imaging, we used a Lumen Dynamics X-Cite120 lamp and Chroma YFP fluorescent filter (NA1028). The sample was maintained at 30°C by a microscope incubator. Phase-contrast and yellow fluorescence images were captured at intervals of 5 minutes for 16 hours. The subsequent image analysis was performed with a custom-made MATLAB program (Vanellus, accessible at: http://kiviet.com/research/vanellus.php).

Ploidy and chromosome segregation model: For simplicity, we assumed every cell has the same effective ploidy, i.e. copies of the gene of interest, over the relevant timescale. At each generation, chromosomes must thus undergo one round of replication and be evenly divided between the two daughter cells. In *E. coli*, chromosomes appear to progressively separate as they are replicated and detach last at the terminus(7). We therefore assumed segregation into daughter cells occurs at the most ancestral split in the chromosome genealogy. This assumption is conservative because it implies that mutant chromosomes always remain together, resulting in the fastest possible approach to homozygosity and thus the shortest phenotypic delay. Under this model, ploidy must take the form $c = 2^n$ (for $n = 0, 1, 2, \ldots$), among which the number of mutant copies is $j = 0$ or 2^i ($0 \leq i \leq n$), while the remaining $c - j$ copies are wild-type. Note that other models of segregation are possible, e.g. random segregation in highly polyploid Archaea(23), which would lead to slower approach to homozygosity and corresponding effects on the evolutionary model results.

Simulated fluctuation tests: All simulations and inference were implemented in R. We simulated culture growth in non-selective media with stochastic appearance of spontaneous *de novo* mutations (for details see Supplementary Text, Section 3.1). We assumed a fixed per-copy mutation rate of μ_c per wild-type cell division, such that the per-cell mutation rate is $\mu = c\,\mu_c$ for effective ploidy c. We neglected the chance of more than one copy mutating simultaneously, i.e. mutants always arose with the mutation in a single chromosome copy. The descendants of each *de novo* mutant were tracked individually, with mutant chromosomes segregating as described above and interdivision times either drawn independently from an exponential distribution or constant. We assumed no fitness differences between wild-type and mutant in non-selective media. In the case of c=1 and exponential interdivision times our model corresponds to the standard "Lea-Coulson" model(14,20), which is also the basis of the widely used software FALCOR(35).

Each simulated culture was initiated with 1000 wild-type cells, and after 20 wild-type population doublings, the culture growth phase ended and phenotypic mutants were counted, under the assumption of either complete recessivity (requiring all c chromosomes to be mutant) or complete dominance (requiring at least one mutant chromosome). Assuming (as standard) 100% plating efficiency and no growth of phenotypically wild-type cells under selective conditions, the number of colonies formed on selective plates equals the number of phenotypic mutants in the final culture. The mutant colony counts from 50 simulated parallel cultures were then used to obtain a maximum likelihood estimate $\hat{\mu}$ and 95% profile likelihood confidence intervals of

mutation rate under the standard model, which in particular assumes that a *de novo* mutant and all its descendants are immediately phenotypically mutant. The best-fitting distribution of mutant counts was calculated from the standard model with mutation rate equal to $\hat{\mu}$. While we implemented these calculations in R, calculation of the likelihood under this model has been previously described(19,36) and has also been implemented in FALCOR(35).

Mutation-selection balance: We considered a population with effective ploidy c, in which mutations arise in a proportion $\tilde{\mu} = c\tilde{\mu}_c$ of offspring in each generation. The definition of mutation rate used in the population genetics literature is subtly different from that used in fluctuation analysis and thus given different notation here (see Supplementary Text, section 4.2). The mutation has relative fitness cost s in homozygotes, with the cost either completely masked (if recessive) or equal (if dominant) in heterozygotes. We extended deterministic genotype frequency recursions to incorporate chromosome segregation as described above, and solved for the equilibrium frequencies of all heterozygous and homozygous mutant types (Supplementary Text, section 4.2).

Evolutionary rescue: We modeled the fate of a population shifted to a harsh new environment, i.e. either extinction or rescue by mutants, stochastically using a multi-type branching process. Unlike in the fluctuation test simulations, where we neglected the chance that wild-type cells produce surviving lineages in the new environment, here we allowed a probability $p_S \leq ½$ that a phenotypically wild-type cell successfully divides before death to produce two offspring, while phenotypically mutant cells have corresponding probability $p_R > ½$. ("Antibiotic efficacy" is correspondingly defined as 1-p_S or 1-p_R.) Thus phenotypically wild-type cells cannot sustain themselves, but have a non-zero chance of producing phenotypically mutant descendants either by segregation of mutant alleles in the standing genetic variation (SGV; modeled by mutation-selection balance as above), or *de novo* mutations during residual divisions in the new environment. We derived analytical approximations (Supplementary Text, section 4.3) for the probability of rescue from SGV (P_{SGV}) or from *de novo* mutations (P_{DN}), which are not mutually exclusive.

Acknowledgements

We thank Erik Wistrand-Yuen, Erik Lundin and Gerrit Brandis from the groups of Dan I. Andersson and Diarmaid Hughes at Uppsala University for kindly gifting us some bacterial strains and plasmids. We also thank Sébastien Wielgoss, Gabriel Leventhal, Andrew Read and Min Wu for helpful discussions.

Financial disclosure

This work was supported by the ETH Zurich; the European Research Council under the 7th Framework Programme of the European Commission (PBDR: grant number 268540 to SB); and the Swiss National Science Foundation (grant number 155866 to SB and grant number 31003A_149267 to MA).

Author Contributions

Conceptualization: Lei Sun, Helen K. Alexander, Martin Ackermann, Sebastian Bonhoeffer.
Formal analysis: Lei Sun, Balazs Bogos, Daniel J. Kiviet, Helen K. Alexander.
Funding acquisition: Martin Ackermann, Sebastian Bonhoeffer.
Investigation: Lei Sun, Balazs Bogos, Daniel J. Kiviet, Helen K. Alexander.
Methodology: Lei Sun, Balazs Bogos, Daniel J. Kiviet, Helen K. Alexander.

Project administration: Sebastian Bonhoeffer.
Software: Balazs Bogos, Daniel J. Kiviet, Helen K. Alexander.
Supervision: Martin Ackermann, Sebastian Bonhoeffer.
Writing – original draft: Lei Sun, Helen K. Alexander, Sebastian Bonhoeffer.
Writing – review & editing: Lei Sun, Helen K. Alexander, Balazs Bogos, Daniel J. Kiviet, Martin Ackermann, Sebastian Bonhoeffer.

References

1. Luria SE, Delbrück M. Mutations of bacteria from virus sensitivity to virus resistance. Genetics. 1943;28:491–511.
2. Ryan FJ. Phenotypic (phenomic) lag in bacteria. Am Nat. 1955;89(846):159–62.
3. Kendal WS, Frost P. Pitfalls and Practice of Luria-Delbruck Fluctuation Analysis: A Review. Cancer Res. 1988;48:1060–5.
4. Sambrook J, Green MR. Molecular Cloning - A Laboratory Manual 4th Edition. 2012.
5. Trindade S, Sousa A, Xavier KB, Dionisio F, Ferreira MG, Gordo I. Positive epistasis drives the acquisition of multidrug resistance. PLoS Genet. 2009 Jul;5(7):e1000578.
6. Cupples CG, Miller JH. A set of lacZ mutations in Escherichia coli that allow rapid detection of each of the six base substitutions. Proc Natl Acad Sci. 1989;86(July):5345–9.
7. Nielsen HJ, Youngren B, Hansen FG, Austin S. Dynamics of Escherichia coli chromosome segregation during multifork replication. J Bacteriol. 2007;189(23):8660–6.
8. Akerlund T, Nordström K, Bernander R. Analysis of cell size and DNA content in exponentially growing and stationary-phase batch cultures of Escherichia coli. J Bacteriol. 1995;177(23):6791–7.
9. Sharan SK, Thomason LC, Kuznetsov SG, Court DL. Recombineering: a homologous recombination-based method of genetic engineering. Nat Protoc. 2009 Jan;4(2):206–23.
10. Edgar R, Friedman N, Molshanski-Mor S, Qimron U. Reversing bacterial resistance to antibiotics by phage-mediated delivery of dominant sensitive genes. Appl Environ Microbiol. 2012 Feb;78(3):744–51.
11. Hayward RS. DNA Blockade by Rifampicin-Inactivated Escherichia coli RNA Polymerase, and Its Amelioration by a Specific Mutation. Eur J Biochem. 1976;71(1):19–24.
12. Kremers G-J, Goedhart J, van Munster EB, Gadella TWJ. Cyan and yellow super fluorescent proteins with improved brightness, protein folding, and FRET Förster radius. Biochemistry. 2006 May 30;45(21):6570–80.
13. Adiciptaningrum AM, Blomfield IC, Tans SJ. Direct observation of type 1 fimbrial switching. EMBO Rep. 2009;10(5):527–32.
14. Foster PL. Methods for determining spontaneous mutation rates. Methods Enzymol. 2006 Jan;409(5):195–213.
15. Tobiason DM, Seifert HS. The Obligate Human Pathogen,Neisseria gonorrhoeae, Is Polyploid. PLoS Biol. 2006;4(6):e185.
16. Kondo S. A theoretical study on spontaneous mutation rate. Mutat Res. 1972;240(5379):365–74.
17. Ryan FJ, Wainwright LK. Nuclear segregation and the growth of clones of spontaneous mutants of bacteria. J Gen Microbiol. 1954;11(3):364–79.
18. Lederberg J. Aberrant heterozygotes in Escherchia coli. Proc Natl Acad Sci. 1949;35(4):178–84.
19. Zheng Q. Statistical and algorithmic methods for fluctuation analysis with

SALVADOR as an implementation. Math Biosci. 2002;176(2):237–52.
20. Zheng Q. Progress of a half century in the study of the Luria-Delbrück distribution. Math Biosci. 1999;162(1–2):1–32.
21. Lee H, Popodi E, Tang H, Foster PL. Rate and molecular spectrum of spontaneous mutations in the bacterium Escherichia coli as determined by whole-genome sequencing. Proc Natl Acad Sci. 2012;109(41):E2774–83.
22. Otto SP, Whitton J. Polyploid incidence and evolution. Annu Rev Genet. 2000;34:401–37.
23. Markov A V, Kaznacheev IS. Evolutionary consequences of polyploidy in prokaryotes and the origin of mitosis and meiosis. Biol Direct. 2016;11(28):1–22.
24. Orr HA, Otto SP. Does diploidy increase the rate of adaptation? Genetics. 1994;136(4):1475–80.
25. Ribeiro RM, Bonhoeffer S. Production of resistant HIV mutants during antiretroviral therapy. Proc Natl Acad Sci. 2000;97(14):7681–6.
26. Barrett RDH, Schluter D. Adaptation from standing genetic variation. Trends Ecol Evol. 2008;23(1):38–44.
27. Bos J, Zhang Q, Vyawahare S, Rogers E, Rosenberg SM, Austin RH. Emergence of antibiotic resistance from multinucleated bacterial filaments. Proc Natl Acad Sci U S A. 2015;112(1):178–83.
28. Soppa J. Polyploidy and community structure. Nat Microbiol. 2017;2:16261.
29. Angert ER. DNA Replication and Genomic Architecture of Very Large Bacteria. Annu Rev Microbiol. 2012;66(1):197–212.
30. Krašovec R, Richards H, Gifford DR, Hatcher C, Faulkner KJ, Belavkin R V., et al. Spontaneous mutation rate is a plastic trait associated with population density across domains of life. PLoS Biol. 2017;15(8):e2002731.
31. Anderson JB, Sirjusingh C, Ricker N. Haploidy, diploidy and evolution of antifungal drug resistance in Saccharomyces cerevisiae. Genetics. 2004;168(4):1915–23.
32. Santos-lopez A, Bernabe-balas C, Ares-arroyo M, Ortega-huedo R, Hoefer A, Millan AS, et al. A Naturally Occurring Single Nucleotide Polymorphism in a Multicopy Plasmid Produces a Reversible Increase in Antibiotic Resistance. Antimicrob Agents Chemother. 2017;61(2):e01735-16.
33. Sawitzke J a., Thomason LC, Costantino N, Bubunenko M, Datta S, Court DL. Recombineering: In Vivo Genetic Engineering in E. coli, S. enterica, and Beyond. Methods Enzymol. 2007;421(6):171–99.
34. Jones TR, Kang IH, Wheeler DB, Lindquist R a, Papallo A, Sabatini DM, et al. CellProfiler Analyst: data exploration and analysis software for complex image-based screens. BMC Bioinformatics. 2008;9:482.
35. Hall BM, Ma C-X, Liang P, Singh KK. Fluctuation analysis CalculatOR: a web tool for the determination of mutation rate using Luria-Delbruck fluctuation analysis. Bioinformatics. 2009;25(12):1564–5.
36. Sarkar S, Ma WT, Sandri GH. On fluctuation analysis: a new, simple and efficient method for computing the expected number of mutants. Genetica. 1992;85(2):173–9.